Smart Rocking Armour Units

Hofland, Bas; Arefin, Syed Shamsil; van der Lem, Cock; van Gent, Marcel

Publication date
2018

Document Version
Final published version

Published in
Proceedings of the 7th International Conference on the Application of Physical Modelling in Coastal and Port Engineering and Science (Coastlab18)

Citation (APA)
Hofland, B., Arefin, S. S., van der Lem, C., & van Gent, M. (2018). Smart Rocking Armour Units. In *Proceedings of the 7th International Conference on the Application of Physical Modelling in Coastal and Port Engineering and Science (Coastlab18): Santander, Spain, May 22-26, 2018*

Proceedings of the 7th International Conference on the Application of Physical Modelling in Coastal and Port Engineering and Science (Coastlab18)
Santander, Spain, May 22-26, 2018

SMART ROCKING ARMOUR UNITS

BAS HOFLAND[1,2], SYED SHAMSIL AREFIN[1,3], COCK VAN DER LEM[4], MARCEL R.A. VAN GENT[2],

[1] *Delft University of Technology, The Netherlands, b.hofland@tudelft.nl*
[2] *Deltares, The Netherlands, marcel.vangent@deltares.nl*
[3] *Institute of Water Modelling, Bangladesh, sam@iwmbd.org*
[4] *Royal HaskoningDHV, The Netherlands, cock.van.der.lem@rhdhv.com*

ABSTRACT

This paper describes a method to measure the rocking motion of lab-scale armour units. Sensors as found in mobile phones are used. These sensors, data-storage and battery are all embedded in the model units, such that they can be applied without wires attached to them. The technique is applied to double-layer units in order to compare the results to the existing knowledge for this type of armour layers. In contrast to previous research, the gyroscope reading is used to determine the (rocking) impact velocities. Two pioneer measurement series are described. From the readings both the temporal distribution of rocking can be inferred, as well as the spatial distribution. The temporal probability distribution for the rocking events seems logarithmic, with the impact velocity $u_{2\%}$ being in the same order of magnitude as those reported earlier. These measurements indicate that for a randomly placed cube in an armour layer most rocking and most violent impact velocities occur about $2D_n$ under the waterline, instead of around the waterline. Moreover, the wave steepness is seen to have an effect on the rocking intensity. From the measurements with multiple units it can be seen that the measured impact velocity exhibits a large spatial variation among different units at an otherwise equal location.

KEYWORDS: Rocking, concrete armour units, rubble mound breakwater, gyroscope sensor.

1 INTRODUCTION

After the failure of several large breakwaters in the 1970's and 1980's due to breakage of concrete armour units, much research was carried out on the wave-induced motion of, the resulting stresses in, and subsequent breakage of these units (Burcharth, 1992). As the stresses are difficult to measure directly in a scale model, the rocking motion of units is nowadays used for design. Typically the percentage of rocking units is measured, although the direct relation of this ill-defined quantity with unit breakage is not clear. One of the important parameters of rocking behavior is the magnitude of the impact velocity and the stochastic and spatial distribution of this impact velocity. However, with the good interlocking capacity and growing size of single-layer randomly-placed concrete units, rocking often is the governing failure mechanism, see Figure 1.

Figure 1. Broken single-layer units in reality (courtesy Royal HaskoningDHV).

Hence, this paper describes a new and promising method to measure the rocking motion of armour elements that was developed at Deltares and TU Delft. Sensors as found in mobile phones are used to measure the rocking of lab-scale units. The sensors, data-storage, and battery are all embedded in the model units. The technique is applied to double-layer units in order to compare the results to the existing knowledge for this type of armour layers. The technique will be used to assess rocking of single-layer units.

2 LITERATURE

In order to incorporate the strength of the armour unit in the breakwater design procedure, a joint industry research program was performed in the 1980's under the coordination of the Centre for Civil Engineering Research and Codes workgroup C70 (CUR C70). Based on high-frequency, one-component acceleration measurements inside model cube

and Tetrapod units, the impact velocities were determined. Based on these results probability functions of the impact velocities were formulated. These impact velocities were combined with advanced strength models of the concrete of the units. This research program was concluded with the creation of a numerical application known as "Rocking", which computes the probability of breakage of (double layer) armour units for given hydraulic and geometric conditions (CUR, 1989, 1990a, 1990b; Van der Meer and Heydra, 1991).

According to the Van der Meer (1988) stability formula, and assuming a storm duration of 1000 waves and a wave steepness of $s_{om} = 0.02$, the initiation of damage for double layer cubes occur when the stability number is $H_s/\Delta D_n \approx 2.4$. CUR (1989) shows that rocking is initiated for a stability number that is 0.5 lower, or $H_s/\Delta D_n \approx 1.9$.

The probability distribution for impacts of cubes that was formulated (Van der Meer and Heydra, 1991) can be written as:

$$p\left(\frac{v_i}{gD_n}\right) = \exp\left(-\left(\frac{40\left(\frac{v_i}{gD_n}\right)}{\exp\left(-0.4\left|\frac{z}{D_n}\right|\right)} - 2.0\right)\left(\frac{H_s}{\Delta D_n}\right)^{-1}\right) \quad (1)$$

where D_n is the nominal diameter of the armour units, g is the gravitational acceleration, H_s is the significant wave height, z the upward coordinate relative to the mean water surface, v_i the impact velocity, $\Delta = \rho/\rho_u - 1$ the relative submerged density, ρ the density of water, and ρ_u the density of the armour units.

The probability distribution for impacts of Tetrapods can be written as:

$$p\left(\frac{v_i}{gD_n}\right) = \exp\left(-\left(\frac{196\left(\frac{v_i}{gD_n}\right)^{1.43}}{\exp\left(-0.4\left|\frac{z}{D_n}\right|\right)} - 2.0\right)\left(\frac{H_s}{\Delta D_n}\right)^{-1}\right) \quad (2)$$

This probability distribution is mainly due to variation in time, as the measurements on which the formula was based were performed with a single unit. What the distribution of the impact velocity for the different units in the armour layer (at the same elevation) is not clear. The elevation of the units relative to the waterline was found to be of influence, with the largest impact velocities around the waterline, as can be seen in Eqs. (1) and (2).

Besides accelerations, also other measurements are possible to detect the influence of the rocking motion on the breakage of armour units, like a direct measurement of normal force, shear force, and/or moments in a critical cross section of the units (Burcharth, 1992). These measurements are even more difficult, as a single element has many possible failure sections.

Le (2015) performed tests on a schematized set-up with a single hinged cube. The cube was placed both on a flat slope, as well as partly embedded in a flat slope. The rocking impacts were obtained from measurements with a miniature 1-component accelerometer on this cube. In contrast to the CUR research, the acceleration during impact was not resolved, but the acceleration prior to impact was integrated to obtain the impact velocity. This method of determining the impact velocity required a much lower sampling frequency. Even though the setup was highly schematized, it seemed that certain findings by CUR (Van der Meer & Heydra, 1991) about the location of the most rocking and the number of impacts that occur were falsified.

For the more modern single layer randomly placed armour units, that are more stable, rocking becomes an even more critical failure mechanism. Because the measurement of impact velocities and related stresses is very difficult, the guidelines for these units typically state a maximum percentage of rocking events in terms of both number of events per element, and number of elements that move (e.g. Zwanenburg et al., 2013; Garcia et. al, 2013). Garcia et. al (2013) state: "..a clear definition of rocking is not easy to provide and deal with". Zwanenburg et al. (2013) conclude that the largest waves in a storm initiate rocking events, such that $H_{2\%}/\Delta D_n$ is a better indicator for rocking than $H_s/\Delta D_n$.

3 PHYSICAL MODEL TESTS

Miniature 9-axis IMU (inertial measurement unit) sensors were obtained that work with the Arduino software platform (www.Arduino.cc). Tests were performed to test the practical applicability of these sensors in breakwater research. Two test series will be described. Firstly, pioneer tests were performed in the large Delta Basin at Deltares with a stand-alone instrumented model-Tetrapod in a realistic random double armour layer. Secondly, tests were done with 8 instrumented cubes in a random double layer at the TU Delft WaterLab. More information can be found in Arefin (2017).

3.1 Sensors

A 9-axis IMU sensor was used that measures acceleration, rotation rate (gyroscope), and magnetic field (compass). These are the same type of sensors that are typically used in mobile phones. This sensor is part of a stack of circuit boards that include a battery, micro-USB connection, sensors, processor, and SD-card. The total size of the

logger is about 20 x 20 x 20 mm^3. The maximum sampling frequency of the sensors is 100 Hz. A mini-SD card was used to store up to 8GB of data, but this reduced the recording speed considerably.

A magnetic sensor is placed inside the model units in order to be able to switch the sensor on and off without having to open the sensor and remove the unit from the armour layer.

3.2 Signal selection and processing

The way that the measured signals with a rather low sampling frequency are used to obtain characteristic values of the impact velocity is described next. In the CUR research the accelerations during the impacts were measured with a 100 kHz sampling frequency. However, model and scale effects occur during the impact itself (Van der Meer and Heydra, 1991), as the material is usually different, the elasticity of the material does not scale well, and viscous effects on the impact location can be present at small scale. Therefore, in the CUR research, the acceleration during the impact was integrated to obtain the velocity just before impact: the impact velocity, v_i. The required 100 kHz sampling frequency as used in the CUR research is much more than the 100 Hz that is typically the sampling frequency of the standard (mobile phone) IMU sensors that we wanted to use for the present research. Therefore, in a previous research, Le (2016) used the acceleration before the impact in order to determine the impact velocity. Now the accelerations before the impact have to be integrated to obtain the impact velocity. As the accelerations in the movement before the impact are related to the wave period in the order of the 1 s duration, instead of the impact of 1 ms duration, a 100 Hz sampling frequency could suffice. This principle is illustrated in Figure 2.

In the present research, another approach was used. As the typical mode of movement is rotation rather than rocking, it seemed logical to use the gyroscope reading instead of the accelerometer reading. In the typical IMU motion sensors that are available these days a gyroscope is usually also included. A gyroscope measures the angular velocity (not acceleration), so when using this signal no integration is needed, but rather a single (angular) velocity measurement just before the impact. Hence maybe even a slightly lower sampling frequency and easier signal processing is expected, as the required parameter (impact velocity) is measured directly. A typical schematized time variation of angular velocity ω and acceleration a before and during an impact is shown in Figure 2. The vertical dashed lines indicate the required sampling frequency for a direct (angular) velocity measurement of prior to the impact, and the required sampling frequency to resolve the acceleration or angular velocity during the impact.

An additional advantage of using the gyroscope signal over the acceleration signal, is that the acceleration signal is also affected by the gravitational acceleration. In a rotational motion the acceleration is not easily corrected for, as the gravitational vector is rotated. When using a gyroscope, this influence is not present.

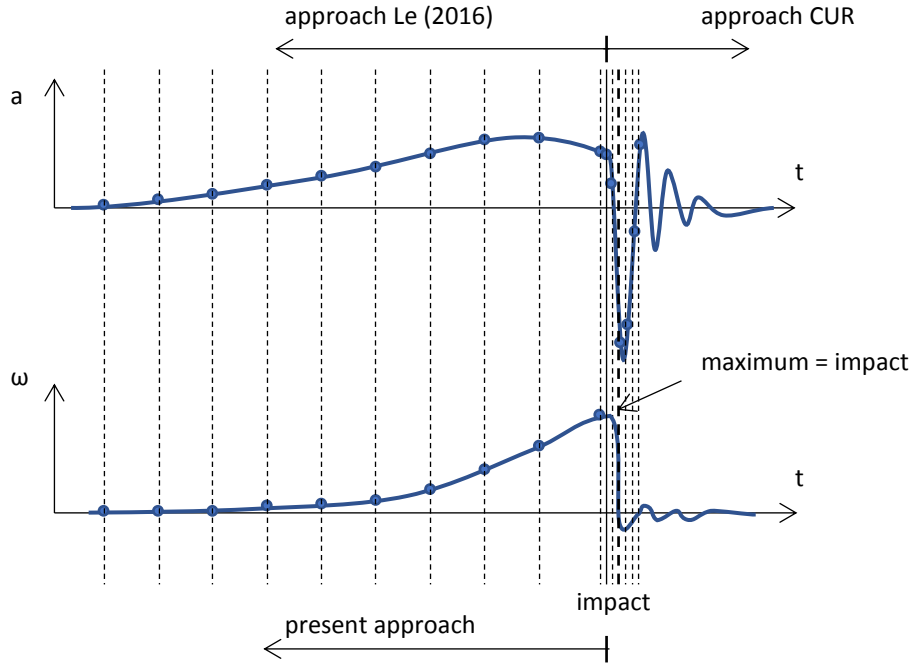

Figure 2. Schematic representation of the time variations of acceleration a and angular velocity ω during rocking and collision (starting at vertical solid line). Dashed lines show sampling times.

The absolute value for the angular velocity is obtained from the three measured angular velocity components (ω_x, ω_y, ω_z) as follows:

$$|\omega| = \sqrt{\omega_x{}^2 + \omega_y{}^2 + \omega_z{}^2} \tag{3}$$

Regarding the peaks of this parameter yields a straightforward way to detect the impact magnitude. Note that in this way both upward and downward impacts will be sensed. Next, the impact velocity is based on these peak angular velocities by assuming a pure rotational motion of the cube, which is the most common mode of movement. The distance between rotation point and impact location is assumed to be about D_n (see Figure 3), so the following relation is used:

$$v_i \approx D_n|\omega| \tag{4}$$

Peaks in the signal above a certain noise threshold are determined from this signal. Next the exceedance curve is made by ordering the impact velocities according to magnitude, in descending order with $v_{i,1}$ being the largest, and the exceedance probability is estimated as:

$$p(v_i > v_{i,n}) = \frac{n}{N_{col}} \tag{5}$$

where N_{col} is the number of collisions in the test. The characteristic impact velocity $v_{i,2}$% is the velocity where the exceedance curve that is found by Eq. (5), has an exceedance probability of 2%.

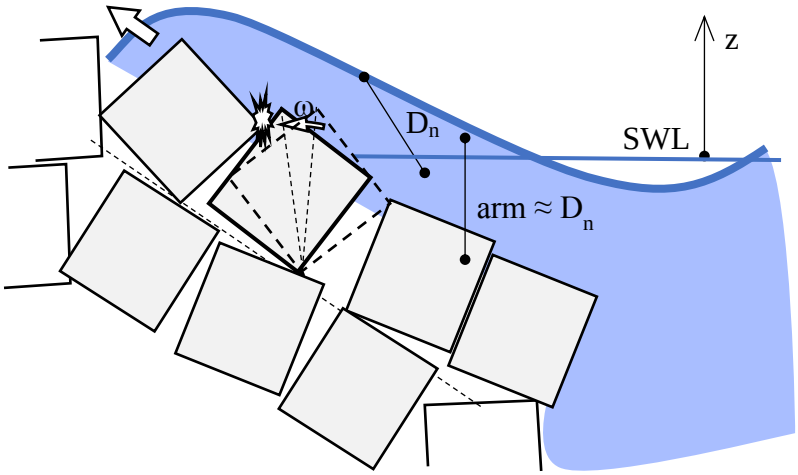

Figure 3. Schematic view of rocking cube in test setup.

3.3 Signal quality and validation

In order to validate the eight sensors used in the second test series, they were placed on a bar that was rotated over 90 degrees. An example of a measurement is given in Figure 4. It can be seen that the gyroscope shows less noise than the accelerometer measurement. The gyroscope measurement shows a slight mean underestimation (bias) of the 90 degree angle of 0.7 degree, and there is some scatter between the various sensors (which could be recalibrated, which has not been done). The noise level is very low. But overall the sensors seem accurate enough.

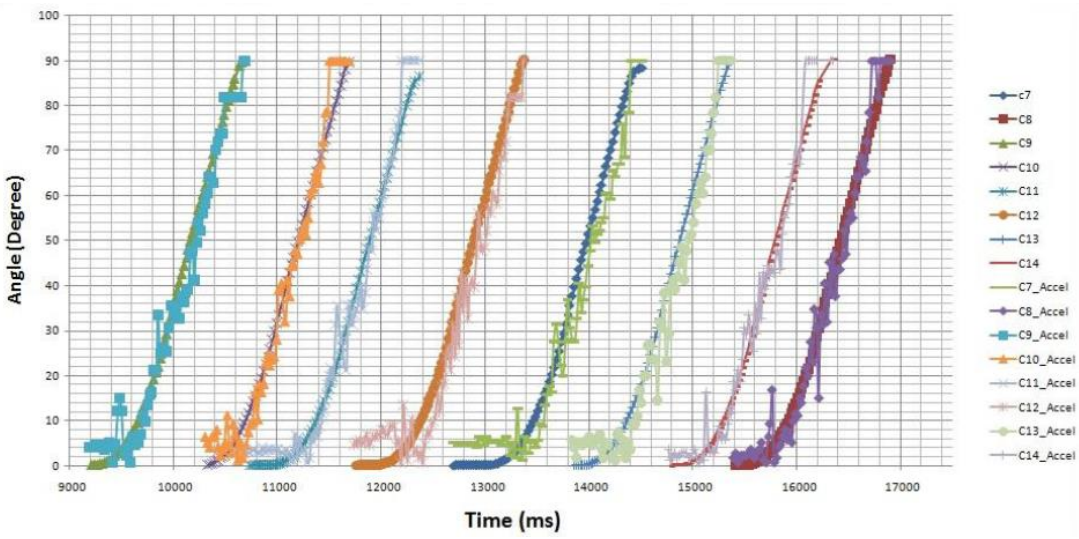

Figure 4. Test recordings with 8 different sensors, integrated gyroscope (solid lines) and doubly integrated accelerometer (lines with markers) readings. Time shifts were applied for clarity.

3.4 Tests with Tetrapod

A first test was performed with a stand-alone instrumented Tetrapod unit made out of two solid pieces of aluminium. The Tetrapod was placed in the model of an ongoing project. The size of the Tetrapod was D = 0.068 m (Figure 5) and the effective density of the unit including the hollow cavity with the logging unit was 2450 kg/m^3, which is similar to the other concrete Tetrapod units used in the model. The tested structure had a 1:1.5 slope and the instrumented Tetrapod was placed at the waterline of a curved section, see right picture in Figure 5. The sampling frequency of the instrument was set to 32.5 Hz to acquire the data.

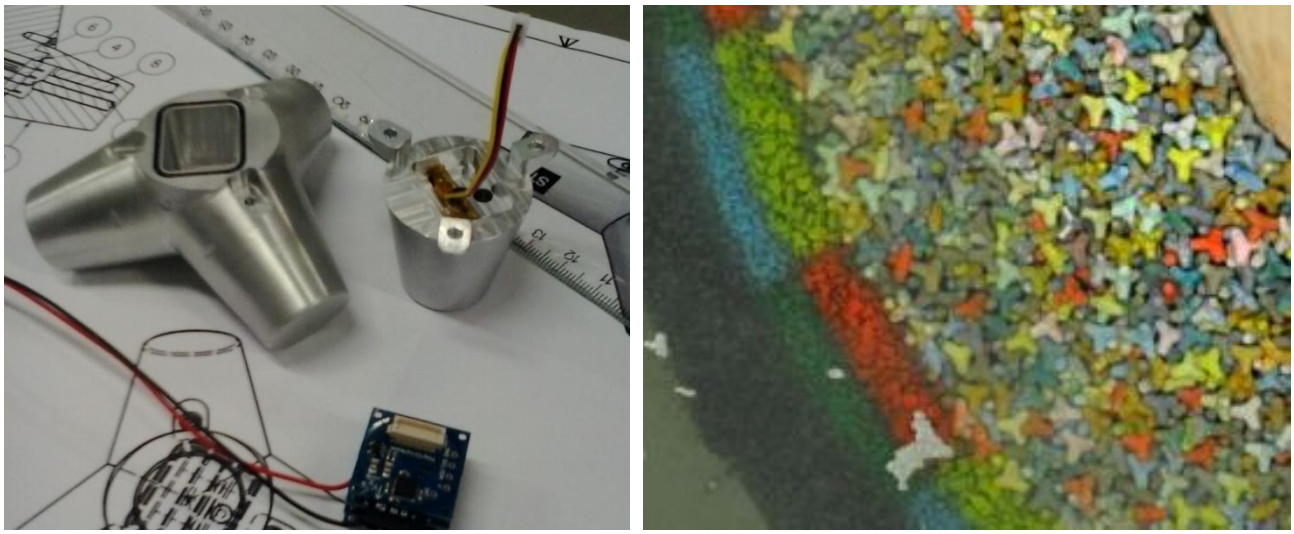

Figure 5. Left: model tetrapod unit with sensor. Right: model tetrapod unit in slope (courtesy Deltares).

Two tests were performed. The irregular wave conditions used during these tests were H_{m0} = 0.09 m; T_p = 1.84s, so s_{op} = 1.7%, and H_{m0} = 0.11 m; T_p = 1.81s, so s_{op} = 2.2%.

3.5 Tests with cubes

In the WaterLab of TU Delft a second experiment was conducted with a 1:1.5 slope of a double layer of randomly placed cubes. The setup is depicted on Figure 6. The cubes which have a nominal diameter of D_n = 4.0 cm and an average density 2464 kg/m^3 were placed on a porous core of gravel with D_{n50} = 2 cm. The core material was bonded by Elastocoast such that the entire core can be placed in the flume quickly in one piece. The slope was placed in front of another setup, at about 15 metres from the wave maker. A set of three resistance type wave gauges was used to measure the wave conditions.

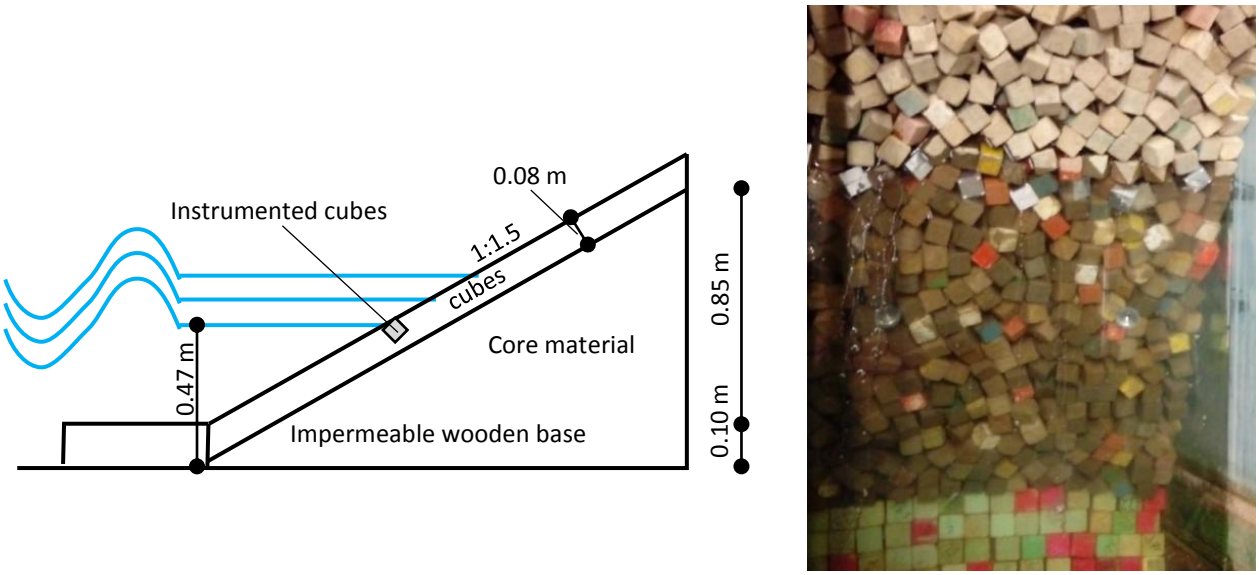

Figure 6. Left: test setup with varying water level. Right: Eight instrumented cubes in model.

During the tests 8 instrumented aluminium cubes were placed next to each other at the same elevation around the waterline. The same sensors were placed in a cavity inside the cubes. Due to the hollow cavity, the effective density of the cubes was close to that of the other model cubes. In this test series the cubes were still connected by a flexible wire in order to increase the testing efficiency (retrieving data and charging the sensors in the units still takes time as the units have to be opened). The data were collected real-time and saved in a text file in a laptop. A sampling frequency of about 50 Hz was applied.

The tests were performed with stability numbers $H_s/\Delta D_n$ up to the initiation of damage, in order to prevent (too many) extractions of cubes. By changing the water level different positions of the cubes relative to the waterline could be obtained: z/D_n=0, z/D_n = -2 and z/D_n = -4 are used during the test program. Three different wave heights and two wave steepnesses were used during this test program, leading to 18 test runs. The test duration was 1000 waves per test. The test programme is given in Table 1.

Table 1. Test programme for cube tests.

Test	H_{m0} (m)	$T_{m-1,0}$ (s)	$s_{m-1,0}$	$H_{m0}/\Delta D_n$	z/D_n	d (m)
1	0.08	1.13	0.04	1.4	0	0.47
2	0.08	1.60	0.02	1.4	0	0.47
3	0.11	1.31	0.04	1.8	0	0.47
4	0.11	1.85	0.02	1.8	0	0.47
5	0.14	1.50	0.04	2.4	0	0.47
6	0.14	2.12	0.02	2.4	0	0.47
7	0.08	1.13	0.04	1.4	-2	0.56
8	0.08	1.60	0.02	1.4	-2	0.56
9	0.11	1.31	0.04	1.8	-2	0.56
10	0.11	1.85	0.02	1.8	-2	0.56
11	0.14	1.50	0.04	2.4	-2	0.56
12	0.14	2.12	0.02	2.4	-2	0.56
13	0.08	1.13	0.04	1.4	-4	0.64
14	0.08	1.85	0.02	1.4	-4	0.64
15	0.11	1.31	0.04	1.8	-4	0.64
16	0.11	1.85	0.02	1.8	-4	0.64
17	0.14	1.50	0.04	2.4	-4	0.64
18	0.14	2.12	0.02	2.4	-4	0.64

4 RESULTS

4.1 Tetrapod

For the tests the impact velocity has been determined by using the angular velocity. In Figure 7 a measurement of the angular velocity and the exceedance curves for both tests are shown. The recordings clearly showed that the impacts peaks due to rocking motion can be distinguished. The exceedance curve for the impact velocities follows a similar distribution as Eq. (2) with impact velocities of a similar order of magnitude. These results from these first tests were encouraging, such that the development was continued.

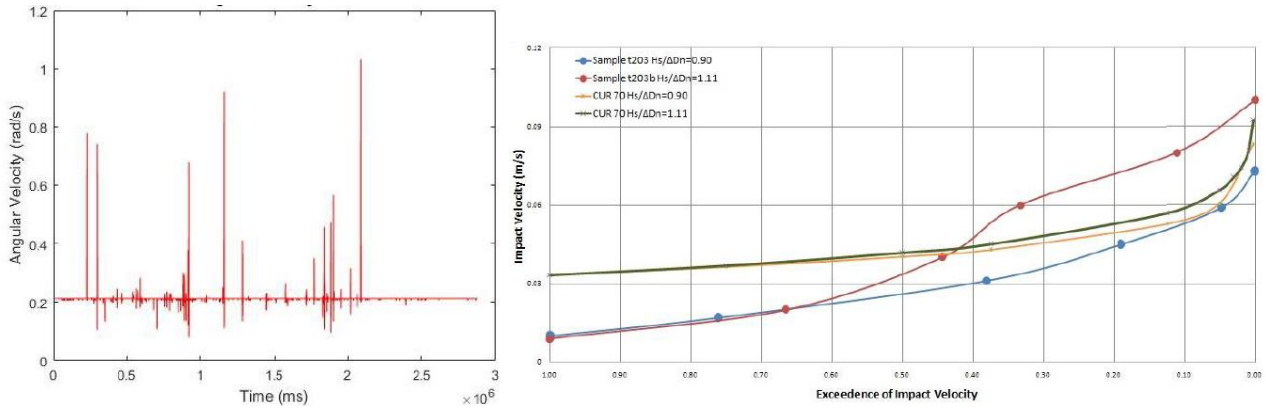

Figure 7. Left: a registration of gyroscope in the model Tetrapod. Right: exceedance curve of the signal compared to Eq. (2).

4.2 Cubes

After the first two tests several instrumented cubes began to malfunction, probably due to insufficient water tightness of the cubes or cables. The last few tests only 4 cubes were still functioning. Also, due to the realistic random placement of the cubes, and the slight settling of the armour layer under wave loading, the local position of the cubes was different for the different cubes, and could also change within or between tests. Results are presented for the four cubes that were seen to move most. It is believed that only when in the order of ten cubes can be instrumented, a sensible estimate of the spatial statistics of the variation in rocking behaviour between cubes at the same elevation – but with a random placement – can be made, so this is not possible yet. During the tests some settlement occured, but no cubes were displaced until Test 17. After this test these cubes were replaced in the slope.

First the number of collisions is treated. The number of collisions is assumed to be equal to the number of peaks in the time signal of the absolute angular velocity $|\omega|$. All peaks above a threshold level of $|\omega| = 0.01$ rad/s are determined. In Figure 8 the number of collisions is plotted as a function of the stability number for the cube that was seen to have the most collisions, cube C4. It can clearly be seen that the number of collisions increases with the stability number, as is expected. This was the case for most cubes, although for some the number of collisions could decrease when the local orientation of the cube and its neighbouring cubes changed due to settlements. Moreover, the number of collisions is largest below the waterline, at the $z/D_n = -2$ location, and the fraction of collisions increases with wave steepness. These trends differ from the CUR research (Van der Meer & Heydra, 1991), but are in line with the findings of Le (2016). It can also be seen that the cube rocks for about 20% of the waves for a stability number $H_s/\Delta D_n = 1.4$, which is much lower than the "initiation of rocking" limit of about 1.8.

In Figure 8 the number of impacts is also consistently larger for the steeper waves with a wave steepness of $s_{m-1,0} = 0.04$. This dependency was also found by Le (2016).

In Figure 9 the number of collisions for four cubes is compared (the four that were functioning during the entire test campaign). Although most trends are the same for all cubes, the number of rocking events shows large variations between the different cubes. This number of impacts, which is in the range of 50% to 100% of the waves for the initial damage level with a stability number around $N_s = 2.4$, is much more than the number of impacts that is found in the CUR research, where a mere three impacts are assumed. The difference can probably be explained by the measurement method. The number of impacts in a naturally placed armour slope was determined in the CUR research using an inventive photographic 'single-frame' technique, where a single picture of the armour layer is made for each rundown event. It might well be that rocking motions where the unit returns to its original position are not detected using such a camera technique. The present technique detects all rocking motions, also when no impact occurs, which might lead to some overestimation of rocking impacts.

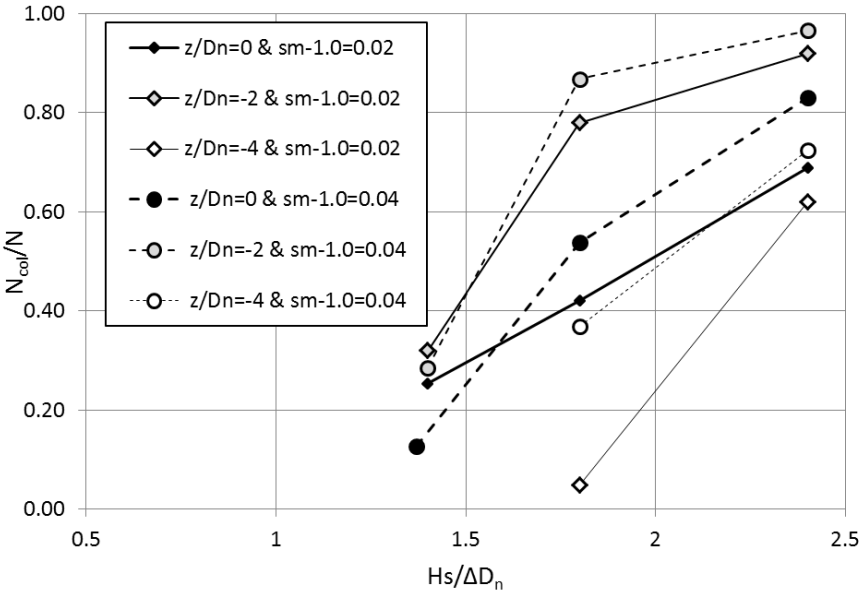

Figure 8. Number of collisions of Cube C4 as a function of stability number $H_s/\Delta D_n$, for various elevations z and wave steepnesses $s_{m-1,0}$.

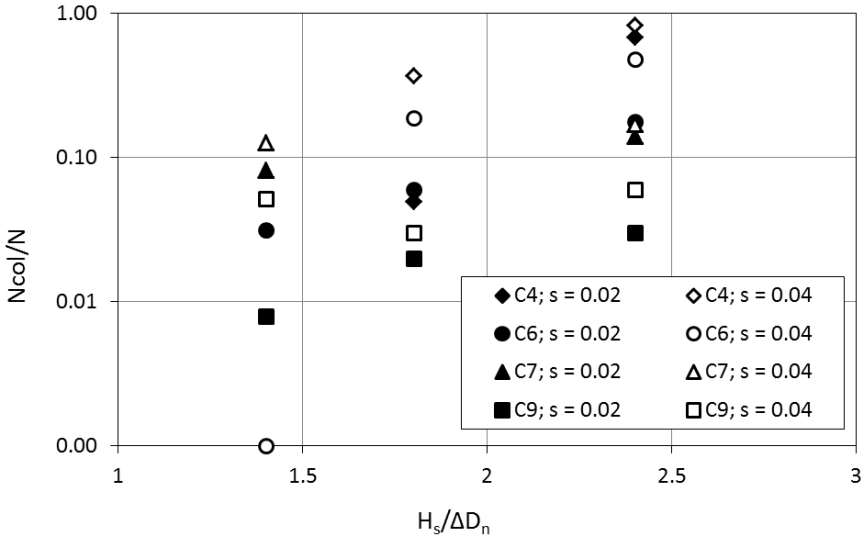

Figure 9. Number of collisions of four different cubes (C4, C6, C7 and C9) for z/D_n = -4.

Now we regard the distribution of the impact velocities. In Figure 10 an example of an exceedance curve for the measured impact velocities for the four different cubes that were rocking (and still functioning) can be seen. It can be seen that the shape of the exceedance curve is roughly exponential for the cube that is rocking most (cube C4), similar to the shape of eq. (1), which is given in the plot as a reference.

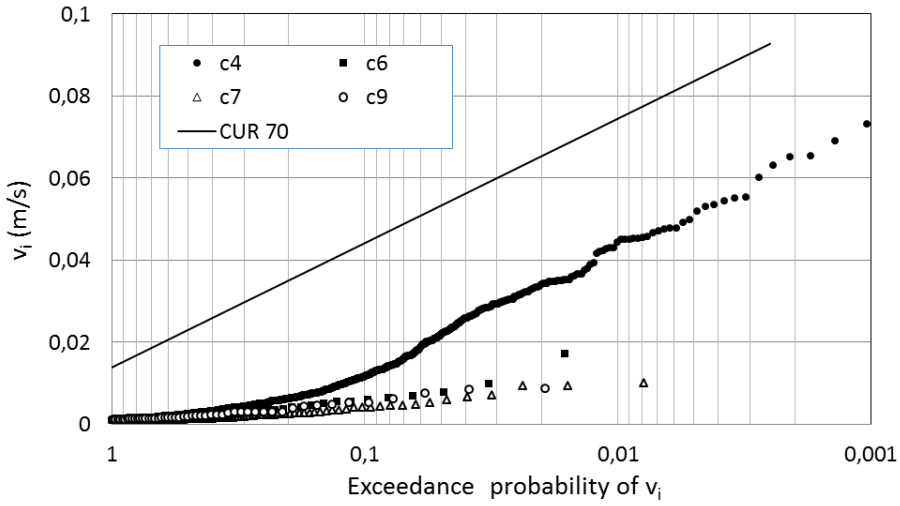

Figure 10. Exceedance curve for impact velocities measured by various cubes for Test 12 ($H_s/\Delta D_n$, = 2.4, z/Dn=-2 and $s_{m-1,0}$=0.02, compared to the distribution of CUR (1990).

From the exceedance curves the characteristic impact velocity due to rocking $v_{i2\%}$, the impact velocity that is exceeded by 2% of the collisions, can be obtained. This value is much smaller than the maximum value in a test with 1000 waves, but statistically more reliable. In Figure 11 theses characteristic impact velocities are given for the different cubes and different positions relative to the water level, z/D_n. The differences between the various cubes are again large, but the impact velocities seem smaller below the waterline, at z/D_n = -2 for most cases and z/D_n = -4 for others. We must be aware that the test programme was such that the cases for z/D_n = 0 were tested first, such that the cubes could have been loosened during these initial tests, which also could yield lower rocking during the first test. However, the tests of Le (2016), who used a fixed setup that did not change between tests also found the largest rocking impact velocities at z/D_n = -2. Hence the results do seem realistic.

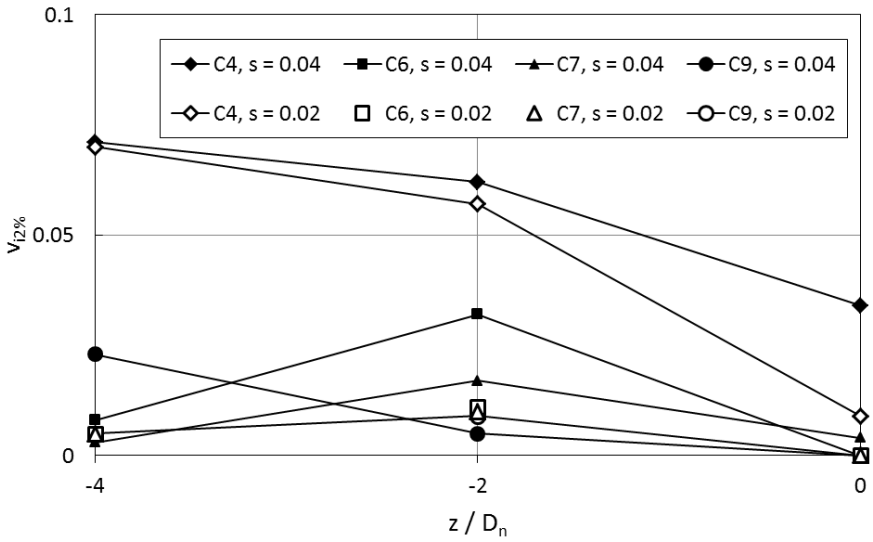

Figure 11. Characteristic impact velocity $v_{i2\%}$ as function of elevation of cubes for $H_s/\Delta D_n$, = 2.4 and different cubes and wave steepnesses.

5 DISCUSSION

In order to validate the new measurement method, tests have been done on similar double-layer units as were tested in previous research. In the future the technique is planned to be applied to single-layer elements.

This paper focussed on a robust and efficient way to determine an important engineering quantity, the characteristic impact velocity of rocking armour units, using modern embedded IMU-sensors. In future analyses we will further develop the analysis of the impacts. In principle the entire motion of the units can be inferred from the signals.

The first thing to add is to distinguish upward and downward impacts, by additionally using the (low-pass filtered) acceleration measurement. The acceleration signal can also be used to distinguish possible translation motion from rotational motion, and might be suited for detecting the impacts.

At the moment for the long-duration stand-alone measurements, the SD card prohibits higher sampling rates than ca. 30 Hz, while the sensors could achieve 100 Hz. Hence the hardware or software will have to be adapted to this end.

As the goal is to instrument large parts of the slope, an efficient way to manufacture many units is sought for. In recent Hydralab+ tests in the wave basin in Hannover 3D printed units have been applied. This approach worked, such that it seems possible to create many instrumented units at reasonable costs. This would open new possibilities for instrumenting entire slopes, and obtain valuable spatial information.

6 CONCLUSION

Experiments were performed in which the rocking motion of model armour units in the wave impact zone were continuously measured by embedding an IMU-sensor and all electronics in the model units themselves. It was found that gyroscope measurements can provide a straightforward measurement of the impact velocity magnitude caused by the impact of a rocking armour unit against an adjacent unit.

The analysis showed that the order of the magnitude of the measured impact velocities is the same as those obtained in the CUR research (1989, 1990-a,b). It was also found that the impact velocity magnitude depends on the wave steepness. Moreover, the number of impacts that was measured was much larger than currently assumed. The number of impacts seems to depend on the wave height, the wave steepness, the vertical position in slope, and the local exposure to wave attack. The latter is a stochastic value that depends on the local random placement of the units. In general the largest number of impacts, and to some extent also the largest impact velocities were found just under the waterline at a vertical level of the (top of the units) of $z/D_n = -2$.

REFERENCES

Arefin, S.S. (2017) *Rocking Revisited 2 - Measurement on Rocking of cubes in a Double Layer on a Breakwater*. MSc Thesis. TUDelft.

Burcharth, H.F. (1992) *Design of rubble mound breakwaters: Structural Integrity*. In: Design and Reliability of Coastal Structures. Short course, 23rd ICCE, Venice.

CUR (1989) *Golfbrekers. Sterkte Betonnen Afdekelementen*. Integratie van Fasen 1-3. Verslag werkgroep 1. Civiel Centrum Uitvoering Research en Regelgeving. In Dutch.

CUR (1990a) *Golfbrekers. Sterkte Betonnen Afdekelementen. Samenvatting onderzoek.* Verslag werkgroep 1. Civiel Centrum Uitvoering Research en Regelgeving. In Dutch.

CUR (1990b) *Golfbrekers. Sterkte Betonnen Afdekelementen. Toepassingen.* Verslag werkgroep 1. Civiel CentrumUitvoering Research en Regelgeving. In Dutch.

Garcia, N., S. Richardson, T. Rigden (2013) *Physical Model Testing of the Hydraulic Stability of Single-layer Armour Units*. Proceedings of the Coasts, Marine Structures and Breakwaters 2013 Conference, ICE. Edinburgh, UK.

Le, T.N. (2016) *Rocking of a single cube on a breakwater slope*. MSc Thesis. Delft: Delft University of Technology

Sokolewicz, M. J. (1986) *Impulsive loads for cubes and tetrapods in consequence of rocking during wave attack*. MSc Thesis. Delft University of Technology. In Dutch: *Impulsbelastingen voor kubussen en tetrapodes als gevolg van rocking bij golfaanval.*

Van der Meer J.W. and Heydra, G. (1991) *Rocking armour units: Number, Location and Impact Velocity*. Coastal Engineering 15, 1991.

Zwanenburg, S.; Uijttewaal, W.S.J., Ten Oever, E., Muttray, M. (2013) *The Influence of the Wave Height Distribution on the Stability of Interlocking Single Layer Armour Units*. Proc. ICE Breakwaters conference. Edinburgh